# Impact of DC Protection Strategy of Large HVDC Network on Frequency Response of the Connected AC System

***D. Zhou*, M. H. Rahman*, L. Xu*, Y. Wang†***

**Department of Electornic & Electrical Engineering, University of Strathclyde, UK (e-mail: ding.zhou@strath.ac.uk, habibur.rahman@strath.ac.uk, lie.xu@strath.ac.uk)*
*†North China Electric Power University, China (email: yi.wang@ncepu.edu.cn)*

**Keywords:** AC-DC grids, AC frequency response, DC fault protection.

## Abstract

Integration of renewable energy generations requires the transmission of bulky power over long distance and HVDC transmission systems become a more preferable choice compared to conventional HVAC systems. For HVDC systems, one of the important concerns is the DC protection strategy which can significantly impact on the connected AC system performance, e.g. system frequency. The maximum loss-of-infeed for a AC network is highly dependent on the duration of the power outage, and the impacts of DC fault protection arrangements which result in different speed of power restoration on the connected AC system, on the system frequency, have not been properly understood. Different DC protection arrangements using DC disconnectors, fast and slow DC circuit breakers on frequency response of the connected AC networks are investigated. A 3-terminal meshed HVDC system is studied to demonstrate system behaviour during DC faults.

## 1 Introduction

High voltage direct current (HVDC) technology has significant advantages on long-distance power transmission and renewable energy integration, e.g. low cost and higher controllability, when compared to the traditional AC power transmission technology. Many HVDC systems have been developed during recent years for network interconnection and offshore wind farm integration. Although most existing HVDC systems are point-to-point projects, forming multi-terminal DC (MTDC) networks is likely to become a common choice when integrating renewable energy cross borders and interconnecting asynchronous AC networks, especially in Europe [1, 2]. The potential increased penetration of MTDC system raises new challenges for AC-DC hybrid system operation and stability that need to be addressed, e.g. system frequency [3].

One major challenge for the system frequency is the decreasing system inertia with large HVDC system penetration which can lead to deteriorated frequency performance under system disturbances. For AC network disturbances such as loss of infeed and load change, it has been indicated in [4-7] that the rate of change of frequency (ROCOF) will increase significantly when the same disturbance occurs in an AC-DC hybrid system with low inertia, compared to the systems with high inertia. In [8], a comparison of frequency response after generator outage in hybrid systems with different levels of wind penetration was carried out and the results showed that the ROCOF and frequency nadir became larger with the decrease of system inertia. Meanwhile, the reduction of system inertia weakens the effect of primary frequency regulation provided by conventional synchronous generators which will make the system frequency performance even worse after such AC network disturbances [9, 10].

In terms of DC network disturbances for an AC-DC hybrid system, the most significant concern is DC fault. However, most of the researches on DC fault in an AC-DC hybrid system have been focused on fault transient analysis, e.g. fault currents [11], fault detection, locating and isolation [12-14], and fault ride-through capabilities [15, 16]. There is limited research on the impacts of DC fault, DC protection strategies and fault ride-through schemes on frequency response of the connected AC system in a low inertia system environment.

In both point-to-point and multi-terminal HVDC systems, DC faults will cause the outage of power transmission between the connected AC networks. This will lead to active power imbalance and cause significant impact on frequencies of those affected AC systems. The severity of the impact is determined by the magnitude and duration of the power imbalance, which is highly dependent on the employed protection strategy and recovery method after fault isolation. Therefore, a better understood of the impact of DC protection and control strategies on frequency response of connected AC network is essential for improving system stability and DC protection technology.

The main objective of this paper is to analyse the impacts of DC protection in a 3-terminal meshed MTDC system on the frequency response of connected AC networks. The rest of the paper is organised as follows. Section 2 recalls a brief description of AC system frequency dynamics under various disturbances. Section 3 illustrates the configuration of the proposed 3-terminal MTDC system and the DC fault protection arrangements which are employed in the case studies. The simulation results and discussions on AC frequency responses under different DC protection strategies are illustrated in Section 4 and finally, Section 5 draws conclusions.

## 2 AC System Frequency Dynamics

Stability of frequency is generally defined as the ability of a power system to maintain or regain a steady frequency after a system disturbance, which depends on the ability of restoring the balance between system demand and generation [17]. Severe system disturbances such as large generation loss and transmission line faults, will lead to significant excursions of system frequency whereas frequency excursion always causes large deviations of voltage, rotor angle and other system variables. Therefore, as one of the most important variable of power system operation and stability, system frequency is always required to maintain at a certain safety range.

The rotor speeds of conventional synchronous generators with rotating mass determine system frequency and they are strictly coupled with the dynamic equilibrium of active power demand and generation. Events of unbalance between load and generation such as unexpected load change and system structure change due to the isolation of faulted elements, will cause frequency excursions. Due to the mechanical nature of system inertia provided by generator rotating mass, frequency excursion dynamic performances are relatively slow which is in the order of hundreds of milliseconds to seconds, compared to other power system transients. The equation connecting active power balance and system frequency excursion is given as:

$$\frac{1}{2}J_{sys}\frac{d\omega^2}{dt} = P_g - P_d \tag{1}$$

where $J_{sys}$ is the system inertia, $\omega$ is the electrical angular frequency, $P_g$ and $P_d$ are system power generated and consumed respectively. For a single generator, the inertia is preferred to be expressed in per unit term as inertia time constant $H_{gen}$ as:

$$H_{gen} = \frac{\frac{1}{2}J_{gen}{\omega_0}^2}{S_{gen}} \tag{2}$$

where $S_{gen}$ is the nominal power rating of the generator, $\omega_0$ is the nominal angular frequency, $J_{gen}$ is the generator inertia. Since system inertia can be simply expressed by the sum of inertias of all generators within the system, therefore the inertia time constant of system can be determined as (3):

$$H_{sys} = \frac{\sum H_{gen} \cdot S_{gen}}{S_{sys}} \tag{3}$$

where $S_{sys}$ is the nominal power rating of the whole system. Since $H_{sys}$ represents the inertia time constant of the whole system, (1) can be rewritten as:

$$2H_{sys} \cdot \frac{d\omega^*}{dt} = {P_g}^* - {P_d}^* \tag{4}$$

where superscript * represents per unit values. It can be seen from (4) that the frequency deviation is determined by system inertia and active power imbalance. The system total inertia is determined by all the generators contained in the system. Thus, for a given system, the inertia is defined and the system frequency is influenced by the system dynamic power balance.

In terms of AC-DC hybrid systems, faults on DC transmission lines will lead to change of system structure and power flow. For a point-to-point HVDC system connecting two AC networks, DC faults will cause severe active power imbalance on both sides due to the loss of the only power transmitting path between the two AC networks. For meshed MTDC system, having multiple interconnected DC transmission lines can provide alternative paths for power transmission in case that one of the DC lines is out of service due to any DC faults. However, the availability of alternative paths for power transmission and arrangement of power re-dispatching are highly depend on the DC protection strategies. For instance, slower DC fault detection and isolation cause longer delay for power re-dispatching through other healthy paths. Therefore, the frequency responses with different DC protection strategies are studied and analysed in this paper.

## 3 System Configuration and Protection

### 3.1 System configuration

The proposed 3-terminal MTDC network is shown in Fig. 1 where Station 1, 2 and 3 are rated at 3GW, 2GW and 1GW respectively. The rated DC voltage is ±400kV. Station 1 acts as the mater DC voltage controller whereas Station 2 regulates active power flowing into the AC Network 2 which contains two synchronous generators SG1 and SG2 with capacity of 2GVA and 1GVA respectively. Station 3 controls its power export from DC to AC Network 3. In this study, the converters are modelled as half-bridge modular multi-level converter (MMC) average model in all three stations [18], and $\pi$ models are used for DC cables with the lengths indicated in Fig. 1.

### 3.2 DC network fault protection

Three different DC fault protection arrangements based on DC switches/disconnectors (DCSWs, which can only open when the current becomes zero) together with AC circuit breakers (ACCBs), fast and slow DC circuit breakers (DCCBs), are tested in the proposed 3-terminal MTDC network. All the three protection arrangements use the same fault locating principle which is introduced in the following sections.

#### (a) Fault locating

Many DC fault locating methods have been studied [11, 13, 14, 19]. A 'Handshaking' approach was proposed in [14], which is the method that employed in this paper to identify and isolate the faulty branch in the proposed system.

With the 'Handshaking' approach, when the DC fault happens, the DC fault current ($I_{dc} > 2\ p.u.$) are labelled depending on its direction by the CBs at each end of the DC cables shown in the Fig. 1. The fault current is positive when flowing into the cable, and negative when flowing out of the cable.

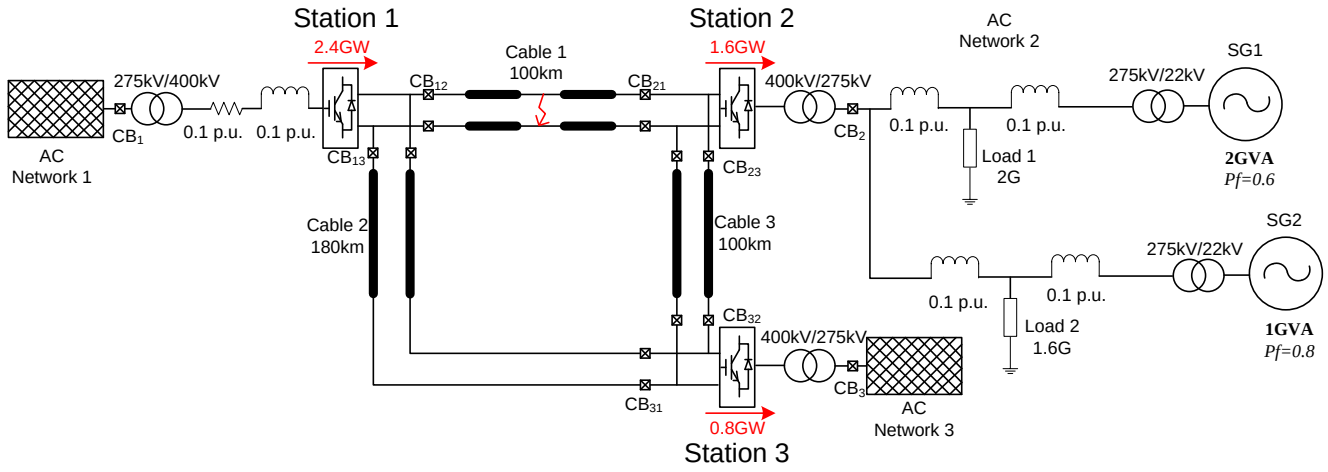


Fig. 1. Block diagram of a three terminal MMC based MTDC network

The cables with fault current labelled as positive at any end are considered as potential faulty lines, and the CBs with fault current labelled as positive are opened to isolate the faulty area. In order to prevent from disconnecting the healthy cables, during the restoring process, the opened CBs will be reclosed when the DC voltage rebuilt on the cable is detected. For an example, when a fault happens on Cable 1 shown in Fig. 1, the DC fault current will be labelled as positive by $CB_{12}$, $CB_{21}$, and $CB_{32}$, and thus Cable 1 and Cable 3 are considered as potential faulty lines, and $CB_{12}$, $CB_{21}$, and $CB_{32}$ are opened. In the restoring process, the $CB_{32}$ will be reclosed when voltage on Cable 3 is rebuilt by Station 2 so as to reconnect the healthy Cable 3 to the network.

**(b) DC protection based on DCSWs**

Under the protection arrangement based on DCSWs, the CBs on each end of DC cables showing in Fig. 1 refer to DCSWs, and $CB_1$, $CB_2$ and $CB_3$ on the AC side of stations are ACCBs. When a DC pole-to-pole short circuit fault happens at the middle of Cable 1, $CB_{12}$, $CB_{21}$ and $CB_{32}$ label the local fault current as positive. Then, all the converters are blocked and the ACCBs, i.e. $CB_1$, $CB_2$, and $CB_3$ are opened, to protect converters and extinguish the fault current flowing into the DC network. When the DC fault current reduced to near-zero, $CB_{12}$, $CB_{21}$, and $CB_{32}$ are opened to isolate the potential faulty cables. Upon isolation of the faulty cables, all the three ACCBs are then re-closed and converters are enabled to recharge the DC network. Because $CB_{23}$ remains closed, the voltage on Cable 3 is rebuilt by Station 2 and detected by $CB_{32}$. Therefore, $CB_{32}$ will be reclosed after the recharge of Cable 3 and brought back online as the healthy branch. However, since the DCSWs can only be opened when the DC current falls to near zero, this protection strategy is relatively slow with the typical recovery time in the order of hundreds milliseconds to a few seconds.

**(c) DC protection based on DCCBs**

In order to quickly isolate the fault and restore the healthy branches, the 'Handshaking' method can be achieved by using DCCBs instead of DCSWs. With the same fault locating method, CBs on each end of DC cables are replaced by DCCBs. Under this protection arrangement, two different DCCB technologies are considered, one based on hybrid type (fast acting DCCB) [20] with a typical opening time of 5ms and the other on mechanical type (slow acting DCCB) [21] with a typical opening time of 20ms. The short duration of such protection process leads to less impact on system frequency of the connected AC networks though the impact of the system recovery speed on acceptable maximum temporary "loss-of-infeed" is largely unknown.

The frequency responses of AC Network 2 showing in the Fig. 1 with the aforementioned three protection arrangements using DCSWs, slow DCCBs and fast DCCBs are studied and discussed in the following section.

## 4 Simulation Results

### 4.1 Typical system behaviour during DC pole-to-pole fault

The typical system behaviour during a DC pole-to-pole fault in the proposed MTDC system showing in Fig. 1 which is protected by DCSWs as described in Section 3.2 (b) is studied.

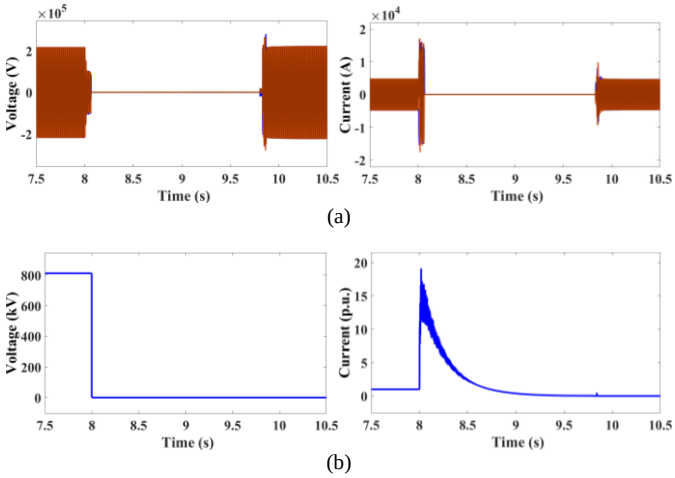


Fig. 2 Typical system response during a DC pole-to-pole fault using DCSW

(a) AC voltage and current at $CB_2$, (b) DC voltage and current at $CB_{21}$

Fig. 2 (a) shows the voltage and current at the AC side of Station 2. When the fault happens at 8s, an AC overcurrent of around 4 p.u. is observed and the current drops to zero after the opening of the ACCBs at 8.06s. Meanwhile, the AC voltage magnitude decreased to half of its normal value due to the connection with faulty branch before being isolated by the ACCBs. Fig. 2 (b) illustrates the current on the DC side of Station 2. As can be seen, it rapidly increases to high value of up to 20 p.u. after the fault initiation as both AC Network 2 and 3 contribute to the DC fault current at $CB_{21}$ through Station 2 and 3, respectively. After the opening of all the ACCBs, the whole DC network is isolated but the de-energisation of the DC network takes considerable time and the DC fault current slowly reduces to zero (over 1s). The DC voltage shown in Fig. 2 (b) dropped to 0 immediately after the fault due to the low impedance on the cables and short distance to the fault location.

### 4.2 System frequency response under the 3 different protection arrangements

Three case studies of the impact of DC fault protection arrangements using DCSWs (Case 1), slow DCCBs (Case 2) and fast DCCBs (Case 3) on frequency response of connected AC Network 2 are carried out in this section. Initially, Station 2 and 3 transmit 1.6 GW and 0.8 GW to AC Network 2 and 3 respectively as indicated in Fig. 1.

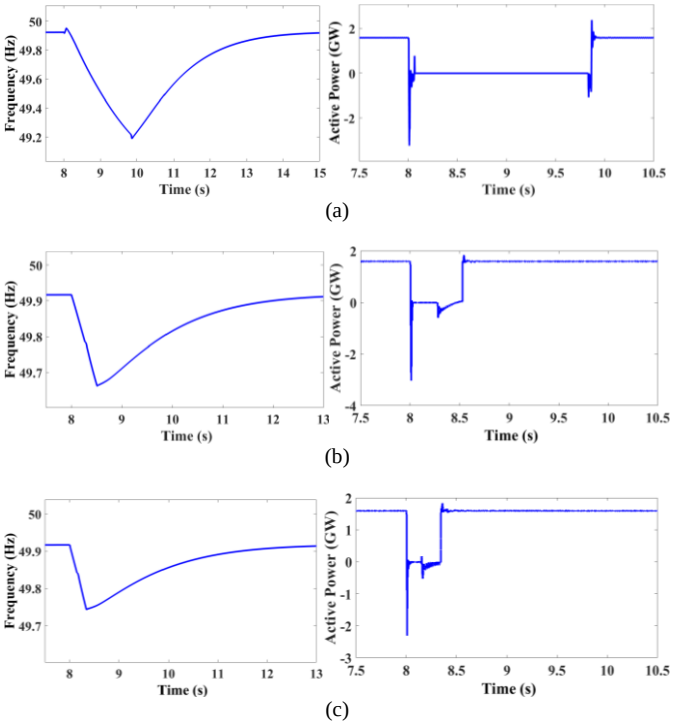


Fig. 3 System response of AC Network 2 during fault isolation and restoration process under different protection strategies after a fault event happened at the middle point of Cable 1 at 8s
(a), (b) and (c) System frequency and active power infeed of AC Network 2 in Case 1, 2 and 3 respectively

In Case 1, the proposed 3-terminal MTDC system is protected using ACCBs and DCSWs as shown in Fig. 1. A permanent DC pole-to-pole fault is applied at the middle of Cable 1 at 8s. Converters at Station 1, 2 and 3 detect the overcurrent flowing through the converter arms ($I_{arm} \geq 2\ p.u.$) and are then blocked at 8.006s, 8.003s and 8.004s respectively, to protect converter components. Meanwhile, Cable 1 and 3 are considered as potential faulty lines by $CB_{12}$, $CB_{21}$ and $CB_{32}$ from the measured DC fault current polarity under the 'Handshaking' principle. The ACCBs, i.e. $CB_1$, $CB_2$ and $CB_3$ are opened 50ms after respective AC overcurrent detection ($|I_{ac}| \geq 2\ p.u.$). Upon the isolation of the AC terminals, the DC network start to discharge, and $CB_{12}$, $CB_{21}$ and $CB_{32}$ are opened at 9.801s as the DC currents on Cable 1, 2 and 3 took considerable time to drop to 20A due to low resistance of the DC cables. Once the faulty branch is isolated, converters at the three stations are de-blocked at 9.841s and start to re-recharge Cable 2 through $CB_{13}$ and $CB_{31}$ and Cable 3 through $CB_{23}$. $CB_{32}$ is re-closed at 9.863s when the magnitude of the DC voltage on Cable 3 is recover to 90% of its normal value. The time sequence of the protection actions are summarised in Table 1.

Table 1 Protection sequence in Case 1

| Events (Case 1) | Time (s) |
|---|---|
| Fault initiation | 8 |
| Blocking of Station 1, 2 and 3 | 8.006, 8.003, 8.004 |
| Opening of $CB_1$, $CB_2$ and $CB_3$ | 8.060 |
| Opening of $CB_{12}$, $CB_{21}$ and $CB_{32}$ | 9.801 |
| Re-closing of $CB_1$, $CB_2$ and $CB_3$ | 9.831 |
| De-blocking of Station1, 2 and 3 | 9.841 |
| Re-closing $CB_{32}$ | 9.863 |

Fig. 3 (a) shows the AC Network 2 frequency and active power infeed to AC Network 2 through Station 2 in Case 1. A reversed overshoot of power infeed is observed at the start of the DC fault due to the large value of AC fault current feeding into the DC network. After the opening of the ACCB at $CB_2$, the active power drops to zero. During the fault protection processes there is no power transmitted to AC Network 2 from 8.06s (i.e. a net loss of 1.6 GW to AC Network 2), and consequently, the frequency at AC Network 2 drops (nadir 49.18 Hz). When Cable 1 is isolated and the system is recovered from fault condition, $CB_{32}$ is re-closed at 9.863s and power transmission restarts. The power infeed to AC Network 2 is now through Cable 2 and 3 instead of Cable 1 and system frequency starts to recover to its normal value in around 5 seconds. The duration of loss of infeed and frequency nadir in Case 1 observed are severe due to the relatively limited synchronous generation in AC Network 2 and large HVDC converter, which is likely to trig load shedding on AC Network 2 according to the current power system code. For such a system, a faster protection strategy is required to reduce the duration of loss of infeed and increase the frequency nadir.

In Case 2 and 3, DCCBs are used with operation times of 20ms and 5ms respectively. The DC fault protection processes of Case 2 and 3 are the same but using different DCCBs with different operation speeds. A permanent DC pole-to-pole fault is applied at the middle of Cable 1 at 8s and Station 1, 2 and 3

are blocked at 8.006s, 8.003s and 8.004s respectively for both cases, after overcurrent on converters arms ($I_{arm} \geq 2\ p.u.$) is detected. DC overcurrent ($I_{dc} \geq 2\ p.u.$) is detected at 8.002s and $CB_{12}$ and $CB_{21}$ are opened with 20ms and 5ms delays for Case 2 and 3, respectively. Similar to Case 1, $CB_{32}$ is also opened and the alternative power transmitting path from Station 1 to Station 2 through Cables 2 and 3 is thus disrupted. Upon the isolation of Cable 1, Station 1, 2 and 3 are de-blocked at 8.28s and 8.15s for Case 2 and 3, respectively, to re-energise Cable 3. Once the DC voltage on Cable 3 is recovered to 90% of its nominal voltage, the $CB_{32}$ is re-closed at 8.53s in Case 2 and 8.345s in Case 3. The power transmitting from Station 1 to Station 2 can then be resumed. The time sequences of the protection actions in Case 2 and 3 are summarised in Table 2.

Table 2 Protection actions in Case 2 and 3

| Events | Time (s) | |
|---|---|---|
| | Case 2 | Case 3 |
| Fault initiation | 8 | 8 |
| Blocking of Station 1, 2 and 3 | 8.006, 8.003, 8.004 | 8.006, 8.003, 8.004 |
| Opening of $CB_{12}$, $CB_{21}$ | 8.022 | 8.007 |
| Opening of $CB_{32}$ | 8.023 | 8.008 |
| De-blocking of Station 1, 2 and 3 | 8.280 | 8.150 |
| Re-closing of $CB_{32}$ | 8.530 | 8.345 |

Figs. 3 (b) and (c) show the frequency and active power infeed of AC Network 2 in Case 2 and 3, respectively. In Case 2, the frequency starts to drop as the result of opening of $CB_{21}$ and $CB_{32}$ which leads to shortage of power infeed to AC Network 2. Fig. 3 (b) indicates that the AC Network 2 frequency drops to around 49.65 Hz. It can also be observed that no active power flows into AC Network 2 between 8.023s and 8.53s. The small negative pulses of active power infeed to AC Network 2 at 8.28s and 8.15s shown in Figs. 3 (b) and (c) are due to the re-charging of Cable 3 after Station 2 was enabled. The faster acting DCCBs equipped in Case 3 can isolate the faulty Cable 1 sooner such that power transmission can be recovered earlier than Case 2 and 1. As a result, the nadir of frequency drop in Case 3 is around 49.75 Hz due to shorter duration of power loss (from 8.008s to 8.345s). Comparing to Case 1, the system frequency performances in Case 2 and 3 are improved and the frequency nadir during DC fault events is increased by the faster fault isolation and system restoration.

Further studies have been carried out to investigate impact of the amount of loss-of-infeed on frequency response during DC fault protection process. This is achieved by setting different initial power infeed from the DC network to AC Network 2 prior to the DC fault. Figs. 4 (a) and (b) show the variation of frequency deviation for different amounts of infeed loss of AC Network 2 during DC fault protection process based on fast DCCBs (with 5ms operation time) and DCSWs respectively.

As can be seen in Fig. 4, the frequency deviation of AC Network 2 increases with the increased loss-of-infeed. On the other hand, it can be observed that for the same frequency deviation, the allowed power loss in Fig. 4 (a) with fast DCCB is much larger than that in Fig. 4 (b) with slow DCSW, e.g. for 0.2 Hz deviation, the allowed power losses are around 1.6 GW in (a) and 0.7 GW in (b), respectively. This indicates that higher power loss can be allowed with faster DC fault isolation and system restoration for the same minimum frequency. Thus, the current maximum 'loss-of-infeed', which is determined based on the amount of permanent power loss, may not be suitable for future AC-DC hybrid power grid. Instead, both the amount of loss-of-infeed and outage duration have to be considered.

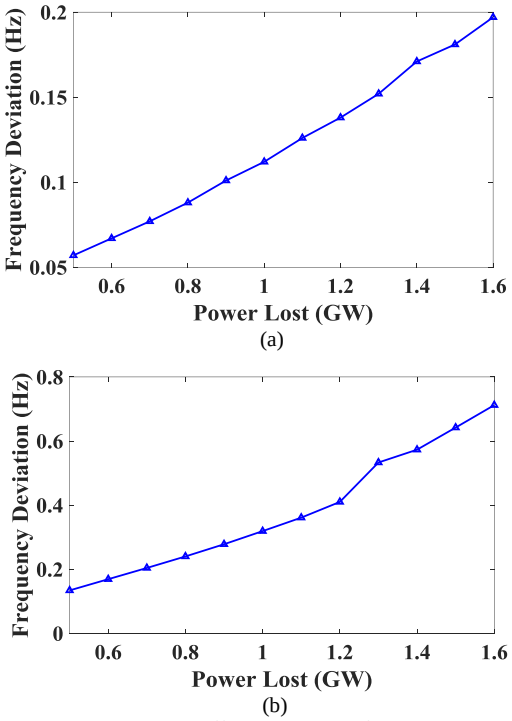


Fig. 4 Frequency response to different amounts of power shortage during DC fault protection processes with alternative protection arrangements: (a) fast DCCBs; (b) DCSWs

## 5 Conclusion

This paper investigates the impacts of different DC fault protection arrangements on frequency response of connected AC systems. A three-terminal meshed MTDC network was modelled and used for case studies. The frequency responses of connected AC network to different DC fault protection arrangements based on DCSWs, slow DCCBs and fast DCCBs were carried out in case studies. It has shown that the frequency performance and frequency nadir are improved with faster DC fault isolation and system restoration. Both the amount of power loss and outage duration affect system frequency response and thus the two need to be considered simultaneously when determining the maximum "loss-of-infeed" for future AC-DC hybrid power grids.

## Acknowledgments

This study is supported in part by the State Key Laboratory of Alternate Electrical Power System with Renewable Energy Sources, China (Grant No. LAPS17010).

## References


[1] D. V. Hertem, M. Ghandhari, and M. Delimar, "Technical limitations towards a SuperGrid--A European prospective," in *2010 IEEE International Energy Conference*, 2010, pp. 302-309.

[2] J. Blau, "Europe plans a North Sea grid," *IEEE Spectrum*, vol. 47, pp. 12-13, 2010.

[3] M. Negnevitsky, D. H. Nguyen, and M. Piekutowski, "Risk Assessment for Power System Operation Planning With High Wind Power Penetration," *IEEE Transactions on Power Systems*, vol. 30, pp. 1359-1368, 2015.

[4] Y. Li, Z. Xu, J. Østergaard, and D. J. Hill, "Coordinated Control Strategies for Offshore Wind Farm Integration via VSC-HVDC for System Frequency Support," *IEEE Transactions on Energy Conversion*, vol. 32, pp. 843-856, 2017.

[5] O. D. Adeuyi, M. Cheah-Mane, J. Liang, and N. Jenkins, "Fast Frequency Response From Offshore Multiterminal VSC-HVDC Schemes," *IEEE Transactions on Power Delivery*, vol. 32, pp. 2442-2452, 2017.

[6] N. R. Chaudhuri, R. Majumder, and B. Chaudhuri, "System frequency support through multi-terminal DC (MTDC) grids," in *2013 IEEE Power & Energy Society General Meeting*, 2013, pp. 1-1.

[7] J. Rafferty, L. Xu, Y. Wang, G. Xu, and F. Alsokhiry, "Frequency support using multi-terminal HVDC systems based on DC voltage manipulation," *IET Renewable Power Generation*, vol. 10, pp. 1393-1401, 2016.

[8] L. Meegahapola and D. Flynn, "Impact on transient and frequency stability for a power system at very high wind penetration," in *IEEE PES General Meeting*, 2010, pp. 1-8.

[9] P. B. Eriksen, T. Ackermann, H. Abildgaard, P. Smith, W. Winter, and J. M. R. Garcia, "System operation with high wind penetration," *IEEE Power and Energy Magazine*, vol. 3, pp. 65-74, 2005.

[10] T. Weissbach and E. Welfonder, "High frequency deviations within the European Power System: Origins and proposals for improvement," in *2009 IEEE/PES Power Systems Conference and Exposition*, 2009, pp. 1-6.

[11] J. Yang, J. E. Fletcher, and J. O. Reilly, "Short-Circuit and Ground Fault Analyses and Location in VSC-Based DC Network Cables," *IEEE Transactions on Industrial Electronics*, vol. 59, pp. 3827-3837, 2012.

[12] C. J. Greiner, T. Langeland, J. Solvik, and Ø. A. Rui, "Availability evaluation of Multi-Terminal DC networks with DC circuit breakers," in *2011 IEEE Trondheim PowerTech*, 2011, pp. 1-8.

[13] M. E. Baran and N. R. Mahajan, "Overcurrent Protection on Voltage-Source-Converter-Based Multiterminal DC Distribution Systems," *IEEE Transactions on Power Delivery*, vol. 22, pp. 406-412, 2007.

[14] L. Tang and B. T. Ooi, "Locating and Isolating DC Faults in Multi-Terminal DC Systems," *IEEE Transactions on Power Delivery*, vol. 22, pp. 1877-1884, 2007.

[15] S. Cui and S. K. Sul, "A Comprehensive DC Short-Circuit Fault Ride Through Strategy of Hybrid Modular Multilevel Converters (MMCs) for Overhead Line Transmission," *IEEE Transactions on Power Electronics*, vol. 31, pp. 7780-7796, 2016.

[16] W. Sanusi, M. A. Hosani, and M. S. E. Moursi, "A Novel DC Fault Ride-Through Scheme for MTDC Networks Connecting Large-Scale Wind Parks," *IEEE Transactions on Sustainable Energy*, vol. 8, pp. 1086-1095, 2017.

[17] P. Kundur, J. Paserba, V. Ajjarapu, G. Andersson, A. Bose, C. Canizares, *et al.*, "Definition and classification of power system stability IEEE/CIGRE joint task force on stability terms and definitions," *IEEE Transactions on Power Systems*, vol. 19, pp. 1387-1401, 2004.

[18] J. Peralta, H. Saad, S. Dennetiere, J. Mahseredjian, and S. Nguefeu, "Detailed and Averaged Models for a 401-Level MMC-HVDC System," *IEEE Transactions on Power Delivery*, vol. 27, pp. 1501-1508, 2012.

[19] T. Lianxiang and O. Boon-Teck, "Protection of VSC-multi-terminal HVDC against DC faults," in *2002 IEEE 33rd Annual IEEE Power Electronics Specialists Conference. Proceedings (Cat. No.02CH37289)*, 2002, pp. 719-724 vol.2.

[20] W. Wen, Y. Huang, T. Cheng, S. Gao, Z. Chen, X. Zhang, *et al.*, "Research on a current commutation drive circuit for hybrid dc circuit breaker and its optimisation design," *IET Generation, Transmission & Distribution*, vol. 10, pp. 3119-3126, 2016.

[21] W. R. L. Garcia, A. Bertinato, P. Tixador, B. Raison, and B. Luscan, "Full-selective protection strategy for MTDC grids based on R-type superconducting FCLs and mechanical DC circuit breakers," in *5th IET International Conference on Renewable Power Generation (RPG) 2016*, 2016, pp. 1-7.